Absorption and Fluorescence of Sm^{2+} in CaF_2, SrF_2, and BaF_2

D. L. Wood and W. Kaiser
Bell Telephone Laboratories, Murray Hill, New Jersey
(Received January 15, 1962)

The absorption and fluorescence of the Sm^{2+} ion have been studied for three host lattices, CaF_2, SrF_2, and BaF_2. Measurements of intensity, linewidth, quantum efficiency, and Zeeman splitting are reported. Energy levels belonging to the $4f$ shell have been identified, and a preliminary analysis of the $4f \rightarrow 5d$ transitions is presented.

INTRODUCTION

In a previous paper[1] (hereafter called I) we have reported on the absorption and fluorescence spectra of CaF_2:Sm^{2+} as well as on experiments with stimulated emission. In the present communication we wish to report on new results for CaF_2:Sm^{2+} and on further studies of Sm^{2+} in the similar host lattices of SrF_2 and BaF_2. From a comparison of the observations on all three systems, we have been able to make a detailed analysis of the spectra, and we have included data relevant to experiments on stimulated emission on all three systems.

EXPERIMENTAL PROCEDURE

The spectra were all measured either with a Cary model 14 double-beam spectrophotometer or a Bausch & Lomb "dual grating" photographic instrument. For most of the absorption data the Cary instrument had adequate resolution, but in a few cases supplementary data were obtained photographically with first-order dispersions of 8 Å/mm or 1.6 Å/mm. The photographic instrument was also used to record the fluorescence spectra with the same dispersions. The Zeeman patterns were obtained in fluorescence using a dc 12-in. electromagnet giving 31 kgauss in a $\frac{3}{4}$-in. gap. The longitudinal Zeeman effect was observed with a small mirror inside the cryostat at 45° to the magnetic field. Fluorescence linewidths were determined by converting microphotometer traces of high-dispersion spectrograms to graphs of emission intensity vs frequency and measuring the half-peak width from the graphs.

The best excitation for fluorescence was obtained with the light from several tungsten lamps used with a blue-green filter. The fluorescence lifetimes were measured by observing the decay with an oscilloscope after excitation with a 1-μsec light pulse from a xenon discharge lamp.

ABSORPTION SPECTRA

The absorption as a function of frequency for the three crystals under discussion are shown in Fig. 1 for a sample temperature of 77°K. The similarities in these three spectra are striking. The red band (at A, B in Fig. 1) occurs at the lowest frequency in CaF_2:Sm^{2+} and has the most pronounced structure in this crystal. In SrF_2:Sm^{2+} the red band is shifted to higher frequency by about 840 cm^{-1}, while in BaF_2:Sm^{2+} the "red" band is actually in the orange and yellow and has essentially no fine structure. The shift is almost 1600 cm^{-1} between CaF_2 and BaF_2 for this band. The blue band (D) shifts in the same direction as the red band and its fine struc-

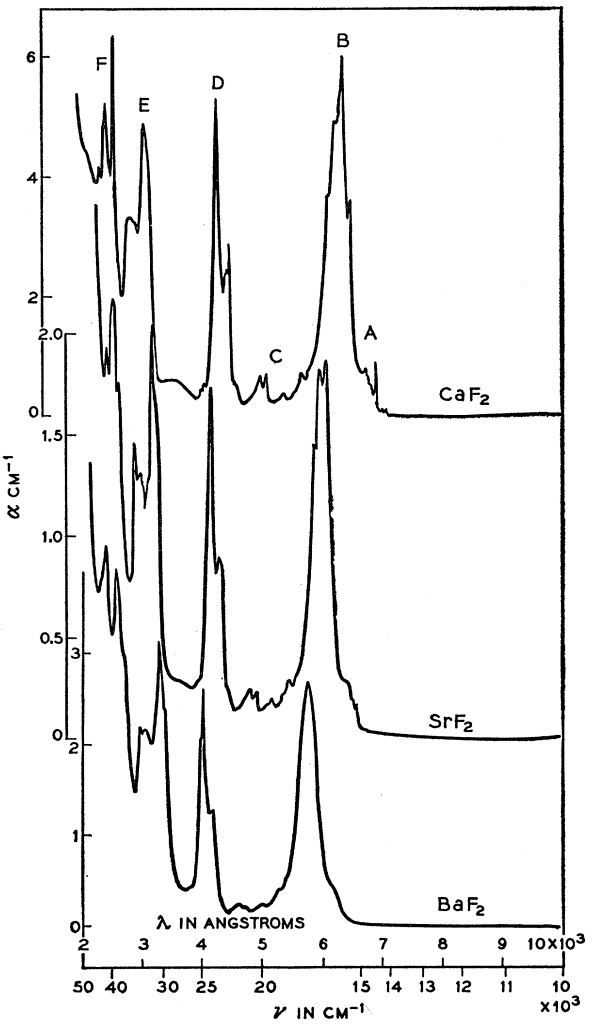

FIG. 1. Typical absorption curves for Sm^{2+} ion in CaF_2, SrF_2, and BaF_2. Ordinates are in units of absorbance α, in cm^{-1} [$\alpha = (1/t)\log_{10}(I_0/I)$]. The Sm^{2+} concentrations in the three samples differ by less than one order of magnitude.

[1] W. Kaiser, C. G. B. Garrett, and D. L. Wood, Phys. Rev. **123**, 766 (1961). Earlier literature on the Sm^{2+} spectrum is cited in this reference.

TABLE I. Selected absorption data at 20°K.

ν (cm^{-1})	$\alpha=D/l$ (cm^{-1})	$\Delta\nu$ (cm^{-1})	f
	$CaF_2:Sm^{2+}$		
14 118 (at 77°K)	21	30	6.9×10^{-4}
14 234 (at 77°K)	13.2	27	3.9×10^{-4}
14 497	1.6	20	3.5×10^{-5}
15 387	7.10	71	5.0×10^{-4}
15 444	7.25	72	5.2×10^{-4}
15 723	10.35		
15 823	9.30		
16 103	8.75	990	9.9×10^{-3}
16 340	6.32		
16 415	5.86		
19 677	1.55	78	1.3×10^{-4}
20 072	1.04	300	3.1×10^{-4}
22 381	5.5	200	1.1×10^{-3}
22 573	4.4		
22 676	3.8	612	2.7×10^{-3}
22 769	4.0		
23 540	8.85	715	6.3×10^{-3}
33 000	7.6	2800	2.1×10^{-2}
35 710	5.0		
39 370	9.0	1100	1.0×10^{-2}
41 841	7.8	2000	1.6×10^{-2}
	$SrF_2:Sm^{2+}$		
14 803 (at 77°K)			
14 925 (at 77°K)			
15 181	1.93	18	3.6×10^{-5}
16 142	5.5	130	6.5×10^{-4}
16 460	10.2		
16 750	9.1	1070	9.6×10^{-3}
20 429	0.71	82	5.8×10^{-5}
20 790	0.97	430	4.2×10^{-4}
23 095	4.1		
23 230	4.4	210	9.2×10^{-4}
23 419	4.4		
24 154	8.4	840	7×10^{-3}
31 056	7.1	1800	1.6×10^{-2}
31 646	8.9		
34 062	5.8		
38 314	7.3		
39 682	9.4	3100	3×10^{-2}
41 494	7.9		
	$BaF_2:Sm^{2+}$		
17 270	6.2	1110	9.6×10^{-3}
23 980	3.5		
24 691	4.9	910	6.2×10^{-3}
24 938	4.0		
30 488	8.5	1950	2.3×10^{-2}
31 949	6.0	5500	4.6×10^{-2}
33 330	5.1		
39 062	9.5		
41 670	10.1		

ture decreases in the same way in the series of crystals. The ultraviolet band (E), on the other hand, shifts from high frequency to lower frequency on going from $CaF_2:Sm^{2+}$ to $BaF_2:Sm^{2+}$, and its fine structure is not greatly different in the three crystals. All bands are considerably broader at 300°K than at 77°K and, although some sharpening of the structure is observed at 4.2°K, no lines disappear at this temperature. The relevant wavelengths, frequencies, absorption coefficients, and oscillator strengths are given in Table I for the three absorption spectra. The accuracy of the oscillator strengths is limited, especially in the case of BaF_2 and SrF_2, because of the difficulty in determining the fraction of Sm in the divalent state. We have used for this purpose the method described in (I) which depends on the change in the Sm^{3+} absorption at 1.2 μ when a colored crystal of known total Sm content is bleached. The bleaching converts all the Sm^{2+} to Sm^{3+} which is colorless. We believe that the red absorption band has a comparable peak absorption coefficient in the three systems, and we have, for convenience, made the assumption that the ratio is unity in calculating the coefficients and f numbers in Table I. We have searched carefully for absorption in $SrF_2:Sm^{2+}$ and $BaF_2:Sm^{2+}$ in the region of the major fluorescence lines, but we

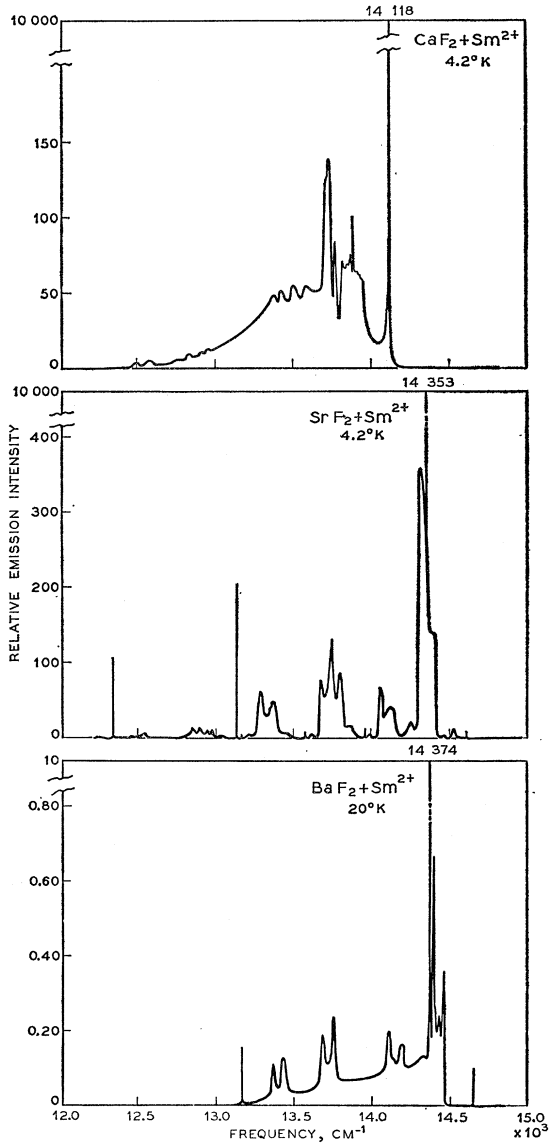

FIG. 2. Fluorescence spectra of Sm^{2+} ion in CaF_2, SrF_2, and BaF_2. Top curve, $CaF_2:Sm^{2+}$ at 4.2°K. Middle curve, $SrF_2:Sm^{2+}$ at 4.2°K. Bottom curve, $BaF_2:Sm^{2+}$ at 20°K. Curves constructed from photographic data. Vertical scales of relative intensity are consistent with each other and with those of Fig. 3. The strongest line is arbitrarily given intensity of 10^4.

have not been able to observe it, even with the heaviest dopings. The importance of this result is explained later. The infrared absorption lines expected for Sm^{2+} have not all been found, probably because their intensity in the highly symmetric site of the CaF_2-type lattice is too small for the Sm^{2+} concentrations we have used, and because our resolving power in the appropriate regions is marginal. In very dark $CaF_2:Sm^{2+}$ containing about 0.75% total Sm, we have observed a very sharp line at 4053 cm^{-1} and another at 2290 cm^{-1}, both of which we believe are due to Sm^{2+}. Their half-widths are about 3 cm^{-1} and both have oscillator strengths of the order of $f=3\times10^{-7}$. There should be another line near 1450 cm^{-1}, and two near 3200 cm^{-1}, but so far they have not been detected. We have taken great care to be sure that the sharp lines observed are not due to Sm^{3+} or to molecular species such as CH and CN often present as impurities.

FLUORESCENCE SPECTRA

The fluorescence spectra for the three systems at low temperature are shown in Fig. 2. These curves have been constructed by making microphotometer traces of spectrograms taken at various exposure times, and reducing these data to relative intensities using the appropriate plate calibration curves. The most intense line has been given arbitrarily an intensity of 10 000 for CaF_2 and SrF_2, while for BaF_2 the intensity of the strongest line has been given a value of 10, since for a uniform, simultaneous, blackbody excitation of all three systems at 4.2°K the emission intensity in the strongest line of $BaF_2:Sm^{2+}$ is about 10^{-3} that of $CaF_2:Sm^{2+}$ and $SrF_2:Sm^{2+}$. The latter have about equal intensity in the corresponding lines. At higher temperatures the ratios are somewhat different (see Table II) with a drastic reduction at 77°K for all three systems. In preparing Table II we have made the simplifying assumption that all three crystals have the same absorption of the exciting light, that the illumination was perfectly uniform, and that the illumination was constant from one temperature to another.

Part of the reason for the decrease of peak intensity of the strong lines at higher temperature is evident from the emission spectra at 77°K shown in Fig. 3. As the temperature rises a continuous background of emission appears and increases in intensity relative to the sharp lines. In addition, the sharp lines broaden, especially in the case of $CaF_2:Sm^{2+}$ causing the peak intensity to

TABLE II. Estimated relative peak intensity of most intense lines in fluorescence.

	$CaF_2:Sm^{2+}$ 14 118 cm^{-1}	$SrF_2:Sm^{2+}$ 14 353 cm^{-1}	$BaF_2:Sm^{2+}$ 14 374 cm^{-1}
4.2°K	10 000	10 000	10
20°K	3500	10 000	10
77°K	100	900	1

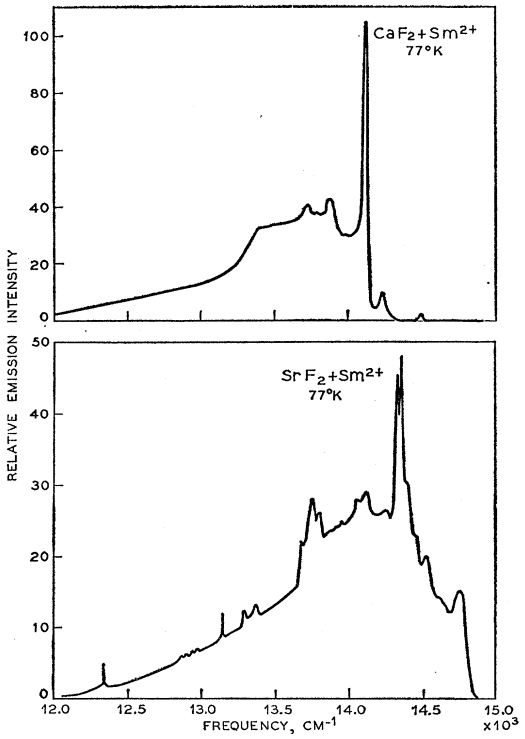

FIG. 3. Fluorescence spectra of Sm^{2+} ion in CaF_2 and SrF_2 at 77°K. Curves constructed from photographic data. Vertical scales of relative intensities are consistent with each other and with those of Fig. 2.

decrease. The efficiency of fluorescence in the sharp lines thus decreases as the temperature increases because of the continuum as we shall point out in the section on quantum efficiency. The spectrum of $BaF_2:Sm^{2+}$ is not included in Fig. 3 because its fluorescence is rather weak at 77°K.

It is important to notice that for $CaF_2:Sm^{2+}$ only one sharp line is observed, with several broader bands on a continuum toward longer wavelength. On the other hand, for SrF_2 and BaF_2 the Sm^{2+} ion emits several very sharp lines in addition to the broad bands. The spectrum of Sm^{2+} in CaF_2 is thus quite different from that in SrF_2 and BaF_2, while the latter two spectra are very similar to each other. This point will be discussed further in a later section. The frequencies of the lines and bands which have been observed in fluorescence are listed in Table III for the three crystals, together with their relative intensities.

EMISSION LINEWIDTH

We have made careful measurements of the dependence of linewidth on temperature for the strongest fluorescence line, and we find that $CaF_2:Sm^{2+}$ has a very much greater increase with temperature than SrF_2 or BaF_2. This shows again that the fluorescence spectrum of Sm^{2+} in CaF_2 is quite different from that in SrF_2 or BaF_2. The relevant data are given in Table IV together

with the frequency, quantum efficiency, and lifetime which are discussed next. The linewidths for $CaF_2:Sm^{2+}$ in Table IV are somewhat smaller than those given in (I), probably due to the improvement in crystal perfection in more recent samples.

QUANTUM EFFICIENCY AND FLUORESCENT LIFETIME

It has been shown in (I) that in $CaF_2:Sm^{2+}$ the whole absorption in the visible and ultraviolet part of the spectrum, especially the strong $4f \rightarrow 5d$ absorption bands, could be used effectively for the population of the metastable fluorescent level. In fact, it was found that the total quantum efficiency, η_t=number of photons emitted in the red/number of photons absorbed, was unity (for 3000 Å$<\lambda<$6500 Å) within an experimental uncertainty of a factor of 1.5. Our data are less extensive for $SrF_2:Sm^{2+}$ and $BaF_2:Sm^{2+}$. A semiquantitative comparison of the three fluorescent materials was made by investigating the fluorescent output of the three crystals CaF_2, SrF_2, and BaF_2 under identical conditions of illumination (tungsten lamp). The crystals were doped with Sm^{2+} to such an extent that a similar absorption strength was obtained. The brightness (intensity times linewidth) of the main emission line of $SrF_2:Sm^{2+}$ was found to be approximately twice that of $CaF_2:Sm^{2+}$ at 20°K (see Tables II and IV) while $BaF_2:Sm^{2+}$ showed an emission 3×10^{-3} times that of the $CaF_2:Sm^{2+}$ crystal. It is of considerable importance to know how much of the total fluorescent intensity is emitted within the major, intense but narrow emission line. As pointed out before, the total red emission covers

TABLE III. Fluorescence.

CaC_2+Sm^{2+}		SrF_2+Sm^{2+}		BaF_2+Sm^{2+}	
$\tilde{\nu}$ (cm^{-1})	Relative intensity	$\tilde{\nu}$ (cm^{-1})	Relative intensity	$\tilde{\nu}$ (cm^{-1})	Relative intensity
14 114 (sharp)	10 000	14 803	0.5		
13 930	62	14 616 (sharp)	11	14 630 (sharp)	0.1
13 915	64	14 530	12	14 465	0.36
13 886	101	14 470	2	14 432	0.24
13 875	76	14 390	140	14 395	0.67
13 855	69	14 325	357	14 374 (sharp)	10
13 825	71	14 260	20	14 331	0.13
13 775	83	14 353 (sharp)	10 000	14 186	0.16
13 735	139	14 125	41	14 118	0.20
13 725	128	14 060	68	13 755	0.24
13 585	55	13 995	2	13 689	0.18
13 500	55	13 964 (sharp)	13	13 432	0.13
13 422	52	13 870	16	13 364	0.11
13 380	49	13 800	86	13 166 (sharp)	0.16
12 920	12	13 750	131		
12 890	10	13 680	77		
12 690	8	13 625	64		
12 620	5	13 581 (sharp)	8		
12 540	5	13 490	1		
12 500	3	13 450	7		
		13 370	50		
14 497 (at 77°K)		13 290	62		
14 234 (at 77°K)		13 230	7		
		13 166 (sharp)[a]	1		
		13 140 (sharp)	205		
		13 062 (sharp)[a]	1		
		13 050	2		
		12 980	11		
		12 950	11		
		12 890	14		
		12 850	14		
		12 780	7		
		12 580	1		
		12 550	3		
		12 520	2		
		12 470	2		
		12 450	1		
		12 350 (sharp)	106		
		12 276	0.5		
		12 246	1		
		12 225[a]	0.2		
		12 146	1.5		
		12 096	0.2		
		12 016	1		
		11 589[a]	0.05		
		11 463[a]	0.09		

[a] Observed only in Ca-doped $SrF_2:Sm^{2+}$.

TABLE IV.

Temperature (°K)	$CaF_2:Sm^{2+}$ $\bar{\nu}$ (cm^{-1})	$\Delta\bar{\nu}$ (cm^{-1})	η_e	τ_{exp} (sec)	$SrF_2:Sm^{2+}$ $\bar{\nu}$ (cm^{-1})	$\Delta\bar{\nu}$ (cm^{-1})	η_e	τ_{exp} (sec)	$BaF_2:Sm^{2+}$ $\bar{\nu}$ (cm^{-1})	$\Delta\bar{\nu}$ (cm^{-1})
90		46				1.1				
77	14 118	21	0.10	2×10^{-6}	14 351.9	0.8	0.03	8×10^{-4}	14 374	1.9
20	14 114	1.1	0.20	2×10^{-6}	14 353.0	0.8	0.4	1×10^{-2}	14 375	1.5
4.2	14 114	0.6	0.35		14 353	0.7	0.4		14 375	1.5

a rather broad frequency range between 14 500 and 12 500 wave numbers. The ratio η_e = number of photons emitted in the main line/total number of red photons, was estimated by integrating the emission spectra shown in Figs. 2 and 3. The value of η_e was found to vary quite strongly with temperature (see Table IV) and reaches a maximum of approximately 40% in SrF_2 crystals (below 20°K). While it appears that $\eta_i \sim 1$ for both $CaF_2:Sm^{2+}$ and $SrF_2:Sm^{2+}$, the latter emits twice as efficiently in the main emission line, and this explains the higher brightness in the comparative experiment mentioned above.

We also have investigated the fluorescent lifetime of the strongest emission line in $CaF_2:Sm^{2+}$ and $SrF_2:Sm^{2+}$. In the first material the experimentally determined value was $\tau_{exp}=2\times10^{-6}$ sec below 77°K. In contrast, a much longer lifetime of $\tau_{exp}=1\times10^{-2}$ sec was found in $SrF_2:Sm^{2+}$ crystals at 20°K; and τ_{exp} decreases strongly around 70°K in this material. The large difference in fluorescent lifetime of Sm^{2+} is in agreement with the change (to be discussed later) in emission character from an electric dipole to a magnetic dipole transition in the host lattices CaF_2 and SrF_2, respectively.

The absorption strength of a transition is related to the radiant lifetime τ by the well-known expression

$$\int \alpha d\nu = \frac{N\lambda^2}{8\pi\tau},$$

where $\int \alpha d\nu$ is taken over the total absorption band, N is the number of ions per cm^3, and λ is the wavelength of the transition. It has been shown in $CaF_2:Sm^{2+}$ for 77°K that the small but clearly measurable absorption at 14 118 cm^{-1} agreed well with the value calculated from $\tau=\tau_{exp}/\eta_e=2\times10^{-6}/0.1=2\times10^{-5}$ sec. In $SrF_2:Sm^{2+}$ the radiant lifetime of the main emission $\tau=8\times10^{-4}/0.03=2.7\times10^{-2}$ sec is larger by a factor of 1300 at this temperature. This large value of τ explains the observation mentioned earlier that no absorption could be detected at 14 353 cm^{-1}, the position of the main emission line in $SrF_2:Sm^{2+}$, since the f number is very small ($f\approx10^{-7}$).

ZEEMAN EFFECT

We have observed the splitting of the Sm^{2+} lines in a magnetic field for various crystallographic orientations, and the Zeeman patterns thus obtained have been very useful in understanding the fluorescence spectra. The crystallographic orientations were easily accomplished using the pronounced (111) cleavage planes as reference directions. The important patterns are summarized in Fig. 4. For $CaF_2:Sm^{2+}$ only the line at 14 118 cm^{-1} is sharp enough to show the Zeeman effect, and this line splits into three components in the field. The pattern is isotropic as far as crystallographic orientation is concerned, and the longitudinal pattern is similar to the $E\perp H_0(\sigma)$ pattern, where H_0 is the applied magnetic field and E the electric field vector of the emitted radiation. In $SrF_2:Sm^{2+}$ there are several lines which are sharp enough for the investigation of the Zeeman effect. Indeed, Zeeman splitting has been observed for several of these. Data have been obtained with polarized light for the lines appearing at 14 353, 13 964, and 13 140 cm^{-1} and each splits into three components with qualitatively similar intensity patterns. The longitudinal patterns for each line correspond to the $E\|H_0(\pi)$ pattern in

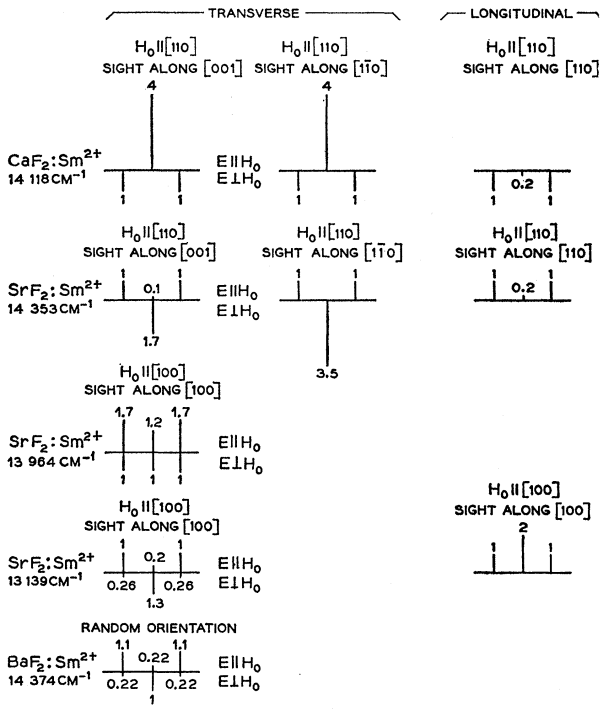

FIG. 4. Zeeman patterns for Sm^{2+} fluorescence in CaF_2, SrF_2, and BaF_2 at 20°K. Only the patterns for lines studied in polarized light are included here. Relative intensities were determined from photographic data. A correction for spectrograph polarization has been applied.

TABLE V. Splitting of the ^7F_J multiplet for Sm^{2+} in SrF_2.

J value	Symmetry species	Emission frequency (cm^{-1})	Relative intensity	Energy level (cm^{-1})	g (calc)	g (obs)
0	$^1\Gamma_1$	14 616 (14 652 in BaF_2)	11	0	0	0
1	$^3\Gamma_4$	14 353 (14 374 in BaF_2)	10[4]	263	1.5	1.4 (same for CaF_2 and BaF_2)
2	$^3\Gamma_5$	13 964	13	652	1.5	2.1
	$^2\Gamma_3$	13 581	8	1035	0	0
3	$^1\Gamma_2$	13 166	1	1450	0	0
	$^3\Gamma_4$	13 140	205	1476	2.25	1.5
	$^3\Gamma_5$	13 062	1	1554	0.75	<0.9
4	$^1\Gamma_1$				0	0
	$^2\Gamma_3$				0	0
	$^3\Gamma_4$	12 350	106	2266	0.75	<1
	$^3\Gamma_5$	12 225	0.1	2391	3.75	~1.3
5	$^2\Gamma_3$				0	0
	$a^3\Gamma_4$	11 589	0.05	3027	2.5	
	$b^3\Gamma_4$	11 463	0.09	3153	3.25	3.25
	$^3\Gamma_5$				3.75	
6	$^1\Gamma_1$				0	
	$^1\Gamma_2$				0	
	$^2\Gamma_3$				0	
	$^3\Gamma_4$	(10 560)[a]		4053[b]	0.75	
	$a^3\Gamma_5$				0.66	
	$b^3\Gamma_5$				4.40	

[a] Not observed in emission.
[b] Observed in absorption for CaF_2.

the transverse effect. The patterns differ with crystallographic orientation in the relative intensities of the π and $\sigma(E\perp H_0)$ components, but the variation is not large.

For BaF_2:Sm^{2+} the fluorescence is so weak that the Zeeman effect has been observed only for the line at 14 374 cm^{-1}. The longitudinal and transverse patterns for this line are very similar to those for the 14 353-cm^{-1} line of SrF_2:Sm^{2+}.

The Zeeman patterns show that the type of transition in CaF_2 is different from those in SrF_2 and BaF_2. In particular, the fact that the longitudinal pattern in CaF_2 is the same as the σ transverse pattern shows that this transition involves an electric dipole. In the case of SrF_2 and BaF_2, however, the longitudinal patterns are similar to the corresponding π transverse spectra, suggesting that these transitions are magnetic dipole in character.

The experimental g values for the observed Zeeman splittings were derived from the formula

$$\Delta\nu=(e/2mc)gH_0=4.67\times10^{-5}gH_0,$$

where $\Delta\nu$ in cm^{-1} is the shift in frequency of a particular component from the zero-field position, and H_0 the applied magnetic field in gauss. The results which are listed in Table V, show that the g factors may be quite different for different levels, and values from $g=0$ to $g=3.25$ were observed. The values in the table are principally for SrF_2:Sm^{2+}, although the few available observations for CaF_2:Sm^{2+} and BaF_2:Sm^{2+} are also noted.

INTERPRETATION OF RESULTS

The Sm^{2+} ion has an electron configuration of $4f^6$ in the ground state, and is therefore isoelectronic with Eu^{3+}. It has already been pointed out in earlier literature[2,3] and in (I) that $4f\rightarrow4f$ transitions like those of Eu^{3+} are expected for Sm^{2+}. In addition, the strong broad absorption bands observed by earlier workers have been attributed to $4f\rightarrow5d$ transitions. We shall begin the analysis of our data by considering first the $4f$ levels of the ground multiplet, which in the free ion are designated ^7F_J. In our experiments, the most complete information on these levels comes from SrF_2:Sm^{2+} where several sharp lines are observed in fluorescence. The positions of the free-ion multiplet levels for Sm^{2+} have been discussed by Butement,[2] and by Dieke and Sarup,[4] and it remains to identify the various levels derived from the free-ion terms as they are affected by the cubic crystal field of the fluorite lattice.

It is known that the cation site in the CaF_2 lattice has O_h symmetry with eightfold (bcc) coordination,[5] and the Sm^{2+} ions substituting for the cation of the host lattice therefore have the same symmetry. The number and symmetry type of all the levels expected have been given by Bethe[6] and for convenience we have listed them in Table V together with the frequency assignments which we now wish to discuss.

[2] F. D. S. Butement, Trans. Faraday Soc. **44**, 617 (1948).
[3] P. P. Feofilov, Zapiski Vsesoyuz Mineral Obschestva **85**, 569 (1956); Optika i Spektroskopia **1**, 992 (1956).
[4] G. H. Dieke and R. Sarup, J. Opt. Soc. Am. (to be published).
[5] R. W. G. Wyckoff, *Crystal Structures* (Interscience Publishers Inc., New York, 1951), Vol. I.
[6] H. Bethe, Ann. Physik **3**, 133 (1929).

Because of the presence of a center of inversion, the parity selection rule forbids electric dipole transitions for rearrangements within the $4f$ shell. Only magnetic dipole or forced electric dipole transitions may be observed between $4f$ levels. The latter type of transition involves a lattice vibration in such a way that either the initial or final state of the transition is a level of the vibrational fine structure of the electronic term. The magnetic dipole transitions, which may take place between pure electronic $4f$ terms, therefore locate the energy levels exactly, in contrast with the forced electric dipole transitions which may differ in frequency from the true electronic level separation by one or more vibrational quanta.

The upper state for fluorescence in $SrF_2:Sm^{2+}$ is by analogy with Eu^{3+} the $^5D_0$ level derived from the $4f$ configuration. It is found at 14 616 cm^{-1} in this crystal, and the weak, fluorescence line at this frequency at 4.2°K (Table III, Fig. 2) is the transition from this metastable level to the ground state ($^7F_0\,^1\Gamma_{1g}$). Since the upper state has $J=0$, its crystal field character is the nondegenerate $^1\Gamma_{1g}$, but the selection rules permit only $^1\Gamma_{1g} \leftrightarrow {}^3\Gamma_{4g}$ for magnetic dipole transitions. This makes the 14 616-cm^{-1} transition very weak since $\Gamma_1 \rightarrow \Gamma_1$ is forbidden. No doubt the free-ion selection rule which forbids the transition $J=0 \rightarrow J=0$ also contributes to the weakness of the line even though this rule is not strictly meaningful in the crystal. The next sharp line at 14 353 cm^{-1} is now a permitted transition $(^5D_0)\,^1\Gamma_{1g} \rightarrow (^7F_1)\,^3\Gamma_{4g}$, and has very great intensity because $\Delta J=1$ is also "permitted." The two weak lines at 13 964 and 13 581 cm^{-1} are the symmetry forbidden $(^5D_0)\,^1\Gamma_{1g} \rightarrow (^7F_2)\,^3\Gamma_{5g}$ and $^2\Gamma_{3g}$, respectively. We know that the $^3\Gamma_5$ lies lower because it splits in a magnetic field (see Fig. 4), and the $^2\Gamma_3$ may not do so in the cubic point group.

In the $J=3$ manifold there are three lines observed, and the very strong one at 13 140 cm^{-1} corresponds to the allowed transition $(^5D_0)\,^1\Gamma_{1g} \rightarrow (^7F_3)\,^3\Gamma_{4g}$. The other two at 13 166 and 13 062 cm^{-1} are the $^1\Gamma_{1g}$ and the $^3\Gamma_{5g}$, but it is not known which is which because the Zeeman splitting of the $^3\Gamma_{5g}$ level is too small to be observed. The next symmetry allowed transition is the $(^5D_0)\,^1\Gamma_{1g} \rightarrow (^7F_4)\,^3\Gamma_{4g}$ at 12 350 cm^{-1}, a fairly strong line. One other line at 12 225 cm^{-1} also belongs to the $J=4$ manifold, but it is not known which one it is. The two $^3\Gamma_{4g}$ levels for $J=5$ correspond to the lines observed at 11 589 and 11 463 cm^{-1}, and the $^3\Gamma_{4g}$ for $J=6$ has not yet been found in fluorescence.

The locations of nine levels of the ground manifold are therefore precisely determined by taking differences between the frequencies of the appropriate emission lines. The positions of the centers of gravity of the groups of levels belonging to the various J's are in very good agreement with those found by Dieke[4] in $LaCl_3$.

It was found that the symmetry of the Sm^{2+} site in SrF_2 could be lowered by adding 5% of CaF_2 to the melt from which the SrF_2 host lattice was grown. This produced only a very minor change in the energy levels and produced a splitting of the sharpest lines of only about 1 cm^{-1}, but the relative intensities of some of the weaker lines were greatly altered. Of special interest was the appearance of several sharp lines which had previously been too weak to observe because the corresponding transitions were forbidden in the purely cubic site. Thus, by lowering the symmetry we were able to add experimental data on two more levels giving 11 in all out of the possible 21. These are noted in Table V.

There are several sets of broad lines in the $SrF_2:Sm^{2+}$ emission spectrum, in addition to the sharp lines discussed above. It is possible to account for these as forced electric dipole transitions. Consider in Fig. 2(b) and Table III the groups of lines which appear just to the long-wavelength side of each sharp line. It is possible to distinguish in most of these groups a progression of peaks with an average spacing of 90, 140, 216, 282, and 349 cm^{-1} from the sharp line. We believe that these progressions correspond to the vibrational frequencies participating in forced electric dipole transitions within the $4f$ level system and that the total fluorescence spectrum arises therefore from both electric and magnetic dipole transitions. The series of broad lines with separations just noted describe the vibrational fine structure of each electronic level.

In $BaF_2:Sm^{2+}$ the magnetic dipole transitions we have identified with $(^5D_0)\,^1\Gamma_{1g} \rightarrow (^7F_0)\,^1\Gamma_{1g}$, $(^7F_1)\,^3\Gamma_{4g}$, and $(^7F_3)\,^3\Gamma_{4g}$ are observed at very nearly the same frequencies as for the case of $SrF_2:Sm^{2+}$ (see Fig. 2 and Table III). The lines lie about 23 cm^{-1} higher in frequency in the BaF_2 lattice. The forced electric dipole transitions have again a repeating pattern, which can be observed only for the first two groups of lines. The separations are 186 and 244 cm^{-1} in BaF_2 as compared with 216 and 282 cm^{-1} for SrF_2. The lower vibrational frequencies for the heavier cation in BaF_2 would be expected.

It is worth noting that these forced electric dipole transitions are separated from the magnetic dipole transitions by very nearly the reststrahlen frequencies of the respective host lattices. Preliminary data[7] show that for SrF_2 the transverse optical mode is observed near 217 cm^{-1} compared with 216 cm^{-1} noted above. For BaF_2 this mode lies at 185 cm^{-1} in the infrared compared with 186 cm^{-1} observed here.

In CaF_2, on the other hand, the sharp magnetic dipole transitions are not observed. There is just the one sharp line at 14 118 cm^{-1}, and we have noted already that it is an electric dipole transition. The rest of the fluorescence spectrum consists of a series of broader lines which can be associated with forced electric dipole transitons similar to those described for the other two crystals. Indeed, in $CaF_2:Sm^{2+}$ one of the stronger of the broad lines at 77°K (at 13 870 cm^{-1}) lies about 250 cm^{-1} away from the principal electronic transition, and this com-

[7] W. Kaiser and W. G. Spitzer (to be published).

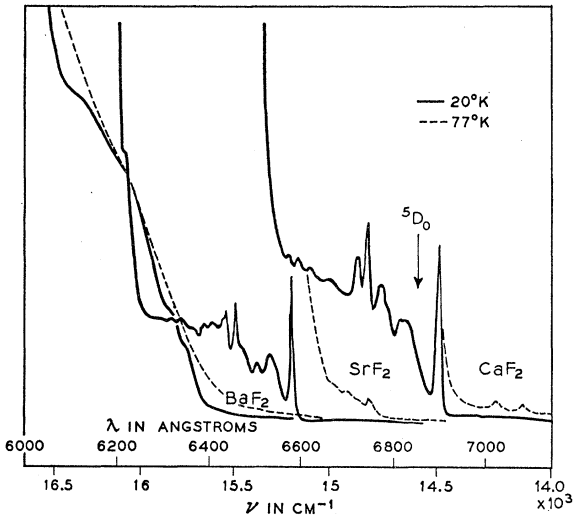

FIG. 5. Details of the absorption spectrum for Sm^{2+} in CaF_2, SrF_2, and BaF_2. The $5d$ absorption lines of Sm^{2+} lie at higher frequency in SrF_2 and BaF_2 than in CaF_2, exposing the $4f\,^5D_0$ level as emitting state for the former two systems. In CaF_2 the $4f\,^5D_0$ is obscured by the $5d$ levels.

pares with the principal reststrahlen frequency of 257 cm^{-1} for CaF_2.

In support of the detailed assignment of the sharp line magnetic dipole fluorescence spectra of $SrF_2:Sm^{2+}$ we call attent on to the Zeeman patterns tabulated in Fig. 4, and the g factors in Table V. Note first that certain lines not included in Fig. 4 such as that at 14 616 cm^{-1} do not split in the magnetic field ($g=0$). This means that the upper emitting level is not affected by the field, and only the terminal states split. This is consistent with the assignment of the upper emitting state to the nondegenerate $^1\Gamma_{1g}$ species of the $^5D_0$ level. The lines at 14 353 and 13 140 cm^{-1} being transitions to $^3\Gamma_4$ species split in the field as they should. The $^3\Gamma_5$ at 13 964 cm^{-1} also splits, consistent with the predictions of theory, while the $^1\Gamma_{1g}$ corresponding to 14 616 cm^{-1}, and the $^2\Gamma_3$ corresponding to 13 581 cm^{-1} do not split as expected. The 12 350-cm^{-1} line was not observed to split in a magnetic field even though all Γ_4 species should do so. On calculating the g factor for this line, we find that the splitting should be about equal to the linewidth (2.17 cm^{-1} in 31 kgauss), and thus it was not observed.

We have calculated the rest of the g factors for the Zeeman effect for all of the levels of the ^7F_g multiplet in the cubic field. The calculation was performed in first order by computing directly the values of the matrix elements of the magnetic perturbation term in the Hamiltonian, $H^m=(e/2mc)H_0(L+2S)$. The wave functions used were obtained by taking linear combinations of free ion functions characterized by the quantum numbers J and M and adjusting the coefficients to agree with the symmetry character of the level in question. Our functions agree with those tabulated by Satten and Margolis.[8] If we assume that the mixing of levels having different J is small, then

$$\begin{aligned}\langle\gamma SJ\Gamma|H^m|\gamma SJ\Gamma\rangle &= (e/2mc)H_0\sum a_i^{\Gamma}\langle\gamma SJM|L+2S|\gamma SJM\rangle \\ &= (e/2mc)H_0\sum a_i^{\Gamma}\langle\gamma SJM|M+S_z|\gamma SJM\rangle \\ &= (e/2mc)H_0 g(SJ\Gamma),\end{aligned}$$

and the values are easily calculated from

$$\langle\gamma SJM|M+S_z|\gamma SJM\rangle = M\left(1+\frac{J(J+1)+S(S+1)-L(L+1)}{2J(J+1)}\right).$$

The results, together with the experimental values observed for $SrF_2:Sm^{2+}$, are collected in Table V, and reasonable agreement is observed. The difference between experimental and calculated g value indicates the degree of mixing of wave functions belonging to different J values. We have neglected this, though it must be appreciable, since this is the mechanism of transfer of intensity from the $^7F_1\,^3\Gamma_{4g}$ line to other lines in the spectrum.

We turn now to the fluorescence spectrum of Sm^{2+} in CaF_2 which is very unlike that in SrF_2 and BaF_2. In the first place, at 4.2°K the very strong, sharp line at 14 118 cm^{-1} is quite far removed from the 14 353 or 14 374 cm^{-1} of SrF_2 and BaF_2. This difference is much too great to arise from the effect of the small change in crystal field between CaF_2 and SrF_2 on a $4f$ level. Secondly, we have shown by comparing the longitudinal and transverse Zeeman effects that the line arises in CaF_2 from an electric dipole transition rather than the magnetic dipole transition observed in the other two crystals. We believe, therefore, that the upper emitting state of the Sm^{2+} in CaF_2 is different from that in SrF_2 and BaF_2.

It seems likely that the upper state has appreciable, perhaps predominantly, $5d$ character and is therefore of u parity, in contrast with the $^5D_0$ upper state in SrF_2 and BaF_2. This would explain the fact that the line is an electric dipole transition in CaF_2, since $u\rightarrow g$ is permitted for this type of transition. The energy shift of the upper emitting state from CaF_2 to the other two crystals would then be due to the much greater sensitivity to crystal field for $5d$ levels compared with the $4f$ levels. Additional support for this contention may be derived from two sources. First, it is a fact that the first two levels of the ground manifold of Sm^{2+} in CaF_2 were found in (I) to have a separation of 263 cm^{-1} compared with 263 in SrF_2 and 256 cm^{-1} in BaF_2. The ground terms are therefore insensitive to the field, and the shift of the fluorescence line must come from the displacement of the upper level. Second, we have investigated the fluorescence in a crystal of $CaF_2:Sm^{2+}$ containing about 2% SrF_2. In this system the sharp

[8] R. A. Satten and J. S. Margolis, J. Chem. Phys. **32**, 573 (1960).

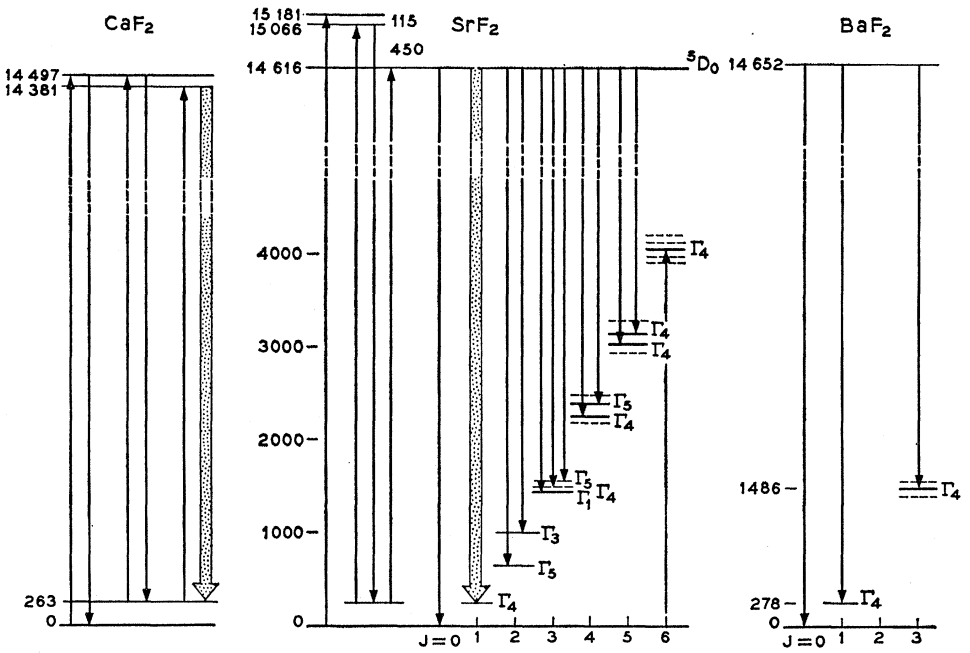

FIG. 6. Comparison of the lower energy levels (in cm^{-1}) of Sm^{2+} in CaF_2, SrF_2, and BaF_2 as determined in this work. Transitions to dashed levels are forbidden and are not observed. Transitions in absorption or fluorescence which have been observed and identified are indicated by arrows.

emission line at 14 118 cm^{-1} of the pure crystal was shifted 15 cm^{-1} toward higher frequency in the mixed crystal, confirming the strong dependence of the upper level on crystal field. In a similar experiment in which a SrF_2:Sm^{2+} crystal was doped with a few percent of CaF_2, the 14 349 cm^{-1} did not shift appreciably, showing that the upper state is quite insensitive to the crystal field for that system.

It is easy to see how the nature of the upper metastable level changes between CaF_2 and SrF_2 when one considers the absorption spectra of Fig. 5. The many relatively sharp lines shown in Fig. 5 lie on the long-wavelength side of the strong $4f \rightarrow 5d$ red absorption band. The similarity of the absorption patterns for Sm^{2+} in CaF_2 and SrF_2 is striking, in contrast with the fluorescence spectra which are so different. The absorption line at 14 118 cm^{-1} in the CaF_2 spectrum corresponds to the transition from the first excited level of the ground manifold, $(^7F_1)\,^3\Gamma_{4g}$, to the principally $5d$ metastable level in question. This coincides with the strong fluorescence line as discussed in (I). In SrF_2, however, this group of lines appears at higher frequency by nearly 700 cm^{-1}, exposing the $(4f\,^5D_0)\,^1\Gamma_{1g}$ level in the latter crystal as the lowest of the excited states. The position of this $4f$ level is probably the same in both lattices, but it cannot be observed in CaF_2 where the lowest $5d$ level lies lower. Indeed, this explanation for the great difference between CaF_2:Sm^{2+} and SrF_2:Sm^{2+} in fluorescence is supported by the fact that we have observed in some of our plates for SrF_2:Sm^{2+} with very long exposures a fluorescence line at 14 803 cm^{-1} which coincides with the lowest frequency absorption band as in the case of CaF_2. This means that there are really two metastable emitting levels in SrF_2:Sm^{2+}, one at 14 616 cm^{-1} giving essentially all but one of the observed lines, and one at 15 066 cm^{-1} giving only one exceedingly weak emission line. It can be expected that the upper emitting level in SrF_2:Sm^{2+} will not thermalize completely with the $^5D_0\,^1\Gamma_{1g}$ even though it is 700 cm^{-1} away if the $4f$ and $5d$ levels should mix weakly.

We can construct, therefore, the three rather detailed energy level diagrams of Fig. 6 for the lower levels of the three crystals under discussion. Note that our labeling of the upper states for CaF_2:Sm^{2+} in (I) is now quite evidently erroneous, since neither level can come from the $4f\,^5D_J$ manifold.

It now remains to discuss the absorption lines arising from the $5d$ levels, and the nature of the emitting state in CaF_2. Because the $5d$ orbitals extend far out into the space near the ligands, the perturbing effect of the ligands on the Sm^{2+} orbitals is large, and we may use the strong field formalism in the way to be described next, and thus determine the level scheme for the broad absorption bands, Putting together the weak field picture for the $4f$ levels and the strong field picture for the $5d$ levels it is possible to arrive at a composite energy level diagram which gives a reasonable understanding of the system.

In the strong field formalism, the number and type of levels can be determined through symmetry arguments alone by putting the requisite number of electrons into the generic levels produced by the crystal field of given symmetry from the various atomic orbitals. The number and character of the actual levels produced can then be determined by group theory. In the case under consideration we have, from the weak field formalism, the complete system of lower levels arising from the $4f$ orbitals, and the six electrons of Sm^{2+} distributed among

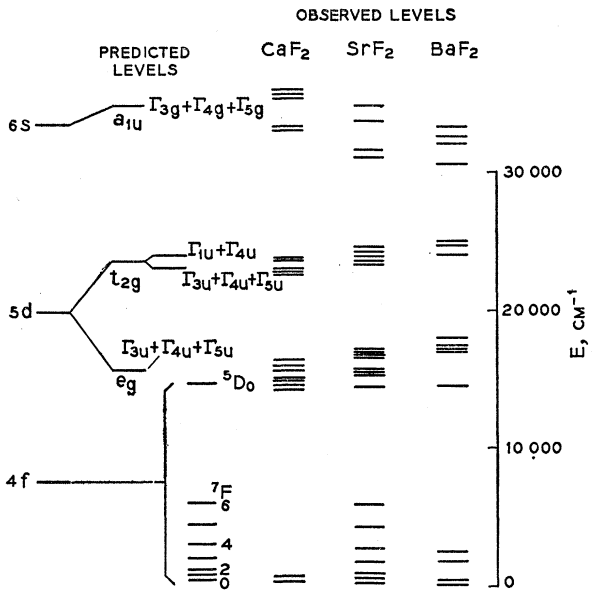

FIG. 7. Energy levels (in cm^{-1}) of Sm^{2+} in CaF_2, SrF_2, and BaF_2. Predicted levels at the left and observed levels at the right. For levels arising within the $4f$ shell the crystal field splitting has been omitted (see Fig. 6).

these levels give the $4f$ terms. Now in addition we have the $5d$, $6s$, and higher orbitals. We know that these, in the bcc configuration, give an e_g level lowest, a t_{2g} next, both from the $5d$, and then the $6s$ gives a simple a_{1g}. Higher terms such as from the $6p$ lie outside the region of experimental observation. It is also easily shown that spin orbit coupling will decompose the t_{2g} into a Γ_7 and a Γ_8 species which would probably have an energy separation of not more than a few thousand wave numbers.

When an electron is promoted from the $4f$ shell to higher levels it leaves behind five electrons in the lowest $4f$ configuration. We know from $Sm^{3+}(4f^5)$ that this is a ${}^6H_{\frac{5}{2}}$ term which in the crystal field divides into a Γ_7 and a Γ_8 of which the Γ_7 lies lower. The first $5d$ level, contains one additional electron (Γ_8) in the e_g component giving the species $(4f^5\,{}^6H_{\frac{5}{2}})\Gamma_7 \times (5d^1)\Gamma_8 = (4f^5 5d^1)\Gamma_3+\Gamma_4+\Gamma_5$. The next levels in a similar way are seen to consist of $\Gamma_3+\Gamma_4+\Gamma_5$, $\Gamma_1+\Gamma_4$ and at high energies $\Gamma_3+\Gamma_4+\Gamma_5$. These levels are shown at the center of the schematic energy level diagram of Fig. 7, and it is now possible to account for the three main broad bands and for at least some of the fine structure of the broad bands because of the multiplicity of levels obtained.

On the right in Fig. 7 are shown the observed levels of Sm^{2+} in the three host lattices. It can readily be seen that the separation of the two groups of $5d$ terms varies much less with the lattice parameter of the host crystal (for CaF_2, $a=5.45$ Å; for SrF_2, $a=5.78$ Å; for BaF_2, $a=6.19$ Å)[6] than the position of the $6s$ levels does with respect to the rest of the levels. This is to be expected, since the $6s$ orbitals extend much farther into space even than the $5d$ and therefore are more sensitive to the changes in environment. The separation of 8000 cm^{-1} between the t_{2g} and e_g levels of the $5d$ seems rather small for a case which is expected to belong to the strong field formalism, and it is entirely possible that the bands near 32 000 cm^{-1} are the t_{2g} levels, with a separation ($10D_q$) of 17 000 cm^{-1} instead. This is a more reasonable value, but the point requires further confirmation. With the former assignment the spin-orbit splitting of the t_{2g} level of the $5d$ is about 2000 cm^{-1}, while the latter assignment would suggest a value of 8000 cm^{-1}, with the two components falling at 16 000 and 24 000 cm^{-1}. It remains to be shown by future work for example with lower symmetries for the Sm^{2+} site whether the choice we have shown in Fig. 7 is the best.

CONCLUSIONS

We have shown that the fluorescence and absorption spectra of Sm^{2+} arise from transitions between $4f$ levels and either $5d$, $6s$, or other $4f$ levels. In fluorescence the CaF_2:Sm^{2+} spectrum consists of a single electric dipole $5d \rightarrow 4_z$ transition together with some vibrational sidebands differing by one vibrational quantum and a continuum. For SrF_2, and BaF_2 the Sm^{2+} fluorescence consists of both sharp magnetic dipole transitions and wider forced electric dipole transitions. The separations between magnetic dipole and forced electric dipole transitions, as expected, correspond to vibrational quanta.

The energy levels of Sm^{2+}, determined experimentally for the three host lattices, can be reconciled in quite fine detail with the levels predicted by crystal field theory for cubal eightfold coordination.

ACKNOWLEDGMENTS

We acknowledge with pleasure the helpful discussions of S. Sugano, H. Kamimura, J. Ferguson, and A. D. Liehr and the very considerable technical assistance of Miss B. E. Prescott. We are very grateful to H. Guggenheim for the preparation of most of the crystals used in this investigation, and to W. A. Runciman for pointing out some numerical errors in the manuscript.